

# **Biochar versus Iron oxide-Biochar performance as adsorbents for Lead and Methyl orange from an aqueous solution**

---

## **ABSTRACT**

Water purification is slowly becoming a problem worldwide due to population growth. Lack of proper wastewater disposal from domestic and industrial sources has escalated water pollution in developing countries. Continuous pollution of water sources has made water purification for domestic supplies very expensive. Modern and cost-effective ways of water purification are urgently needed. One of the modern emerging technologies is adsorption using nano-materials. The aim of the study was to prepare an engineered iron oxide-biochar ( $\text{Fe}_2\text{O}_3\text{-BC}$ ), a nano-composite using pyrolysis and microwave activation. The efficiency of the nano-composite was evaluated in the removal of the heavy metal lead (Pb) and the dye methyl orange (MO) in aqueous solutions. Infrared spectroscopy was used to identify the functional groups present in the synthesized biochars before and after adsorption. The adsorption properties of the synthesised  $\text{Fe}_2\text{O}_3\text{-BC}$  and biochar (BC) were determined by application in lead metal and methyl orange aqueous solutions on known concentrations. FAAS and UV/VIS Spectrophotometry were used for Lead and Methyl Orange concentrations measurements respectively. Batch adsorption experiments were conducted to investigate the capacity of  $\text{Fe}_2\text{O}_3\text{-BC}$  and BC to remove MO and Pb in aqueous solutions. A dose of 50 mg  $\text{Fe}_2\text{O}_3\text{-BC}$  had the highest percentage MO removal of 89.81% at pH 2 while 50 mg of BC had a highest of 11.55% at pH 12. A dosage of 100 mg of  $\text{Fe}_2\text{O}_3\text{-BC}$  had 100% MO removal and 250 mg BC achieved a maximum of 30.61% removal in 30 minutes. Maximum MO removal concentrations were 70 mg/L and 55 mg/L respectively for  $\text{Fe}_2\text{O}_3\text{-BC}$  and BC adsorbents. Both  $\text{Fe}_2\text{O}_3\text{-BC}$  and BC had  $\text{Pb}^{2+}$  removal of 97% in 30 minutes. A dose of 65 mg for both  $\text{Fe}_2\text{O}_3\text{-BC}$  and BC adsorbents had 100% removal of  $\text{Pb}^{2+}$ . The adsorption studies of both MO dye and  $\text{Pb}^{2+}$  on  $\text{Fe}_2\text{O}_3\text{-BC}$  nano-composite fit the Langmuir isotherm ( $R^2$  value of 0.999) and Temkin isotherm ( $R^2$  value of 0.919). The  $\text{Fe}_2\text{O}_3\text{-BC}$  nano-composite adsorbs Pb and MO dye better than biochar. The  $\text{Fe}_2\text{O}_3\text{-BC}$  nano-composite could be a good adsorbent for other cations and anions. More work need to be done in order to investigate the adsorption potential of other cations and anions using  $\text{Fe}_2\text{O}_3\text{-BC}$  nano-composite

*Keywords: Biochar, adsorption, adsorbate, pyrolysis, heavy metal, biosorption, environment*

## **1. INTRODUCTION**

Wastewaters are produced in many industrial processes, mostly from mining, steel mills, tanning plants, production of chemical fertilizers and pesticides, fabric dyeing plants, electroplating plants, motor and power engineering plants, and battery and accumulator

production plants [1,8]. Heavy metals flow into the ecosystem due to civilization and industrial development [2]. The creation of undefined mineral and organometallic linkages in aqueous and land environments can be attributed to heavy metals. In the environment, heavy metals show high mobility. Plant roots take up heavy metals which end up in the digestive systems of humans and animals [6]. Heavy metals pose serious threats to living organisms due to toxic effects on certain elements of the environment and bioaccumulation in the food chain [9]. The methods commonly used for metal ions removal are chemical precipitation, lime coagulation, ion exchange, reverse osmosis and solvent extraction from aqueous streams [31, 40]. New technologies for removal of toxic metals from wastewaters have focused attention to biosorption, because biological materials have strong metal binding capacities. Adsorption technologies are of the most effective methods for dye removal due to its high efficiency, low cost, and easy to perform [36, 37, 38].

Several single solution experiments have been carried out on heavy metal removal [3,13,19], [28] used solid olive solid residues, [18,26,30] used activated sludge, biosorbents and aquatic macrophytes respectively for zinc removal from aqueous solutions. However, it is important to note that wastewaters contain various heavy metals in solution [14,27,33]. It is prudent to carry out experimental work where one or more heavy metal is under study.

Biochar (BC) is prepared by pyrolysis (300°C and above) of a biomaterial in the absence of air until all the organic compounds except carbon are volatilised [12,22]. It has been used for tertiary treatment of municipal and industrial wastewaters [15]. Biochar adsorbs soluble organics namely nitrogen, sulphides and heavy metals in wastewater following biological or physical-chemical treatment [15]. Biochar though effective in adsorption, is limited to wastes with low organic concentrations (less than 5%), low inorganic concentrations (less than 1%) and unable to remove highly soluble organics, or those with low molecular weights [23,25]. To counter BC deficiencies in adsorption, there is need to activate it and enhance it with an oxide. Iron oxide has been used as an adsorbent in several studies in aqueous solutions [2,21,34,39]. However, to increase the number of adsorption sites, activated BC is among the adsorbents available for such studies [4,41,35].

The synthesis of activated biochar using microwaves is an area that needs more investigation because biochar generation from paper and pulp sludge has not received much research attention to date. Some researchers have reported an increase in surface area and porosity on microwave generated biochar, which was accompanied by an increase in the adsorption capacity of the adsorbent [11]. In addition, the smaller the particle size the greater the surface area for adsorption, so the activated BC ground to nano scale is expected to adsorb more [24].

In most cases the biosorption studies focused mainly on single solutions, few on binary solutions and very few on ternary solutions. An activated metal oxide biochar nano-composite represents an emerging group of adsorbents for removal of neutral and ionic contaminants in aqueous solutions [36]. This study focused on preparation of an activated metal oxide biochar nano-composite, characterisation and application in single solutions.

Activated BC has lower adsorption towards anions in solutions and it has been mainly applied to single solutions [4]. It needs modification for efficient removal of anions in single, binary and ternary solutions. A metal oxide biochar nano composite represent an emerging group of adsorbents for removal of neutral and ionic contaminants in aqueous solutions [36]. The main benefits of biosorption over conventional treatment methods are low cost and high efficiency. It also minimise chemical or biological sludge and the biosorbent can be regenerated [5,20]. The biosorption method has been proposed as an effective decolourization method for dye contaminated wastewaters [10, 17, 30, 41]. Chemical methods for heavy metals removal are expensive. Engineered biochar (activated) has got unique properties potentially competent of heavy metal removal and decolourization ability in wastewater, therefore capable of removing dyes [30,39].

## 2. MATERIALS AND METHODS

### 2.1 Chemicals and Materials

The chemicals and materials which were used in this study includes Paper and Pulp Sludge (PPS), KOH analytical grade, HCL, iron chloride ( $\text{FeCl}_3$ ), deionised water, pH meter (Mettler Toledo), Shaker (Merck) and microwave (Samsung).

### 2.2 Preparation of Biochar (BC) and $\text{Fe}_2\text{O}_3$ -BC

The BC and  $\text{Fe}_2\text{O}_3$ -BC were prepared according to the procedure mentioned by [7,11]. Briefly, 500 g of Paper and Pulp Sludge (PPS) obtained from Kadoma Paper Mills was dried at  $105^\circ\text{C}$  for 24hrs. The PPS was pre-ashed to remove volatiles in an oven at  $200^\circ\text{C}$  for 2hrs in an air tight container. The carbonization of the pre-ashed PPS was carried out in a muffle furnace at  $500^\circ\text{C}$  and  $700^\circ\text{C}$  separately for 2hrs. Potassium hydroxide (5 grams) was used to impregnate the biochar (1:2). Deionised water (100 mL) was added to dissolve all the KOH pellets, and the mixture left for 24 hrs at room temperature. Further activation of the impregnated BC was carried out using a microwave (800 watts) for 6 minutes. The sample was then cooled at room temperature and washed with hot distilled water. 12 grams of BC were thoroughly mixed with 4 grams of  $\text{FeCl}_3$ . The mixtures were put in a muffle furnace at  $500^\circ\text{C}$  and  $700^\circ\text{C}$  separately for 2hrs each. The BC and  $\text{Fe}_2\text{O}_3$ -BC samples were ground, sieved through  $250\mu\text{m}$  and stored in a closed container for use.

The percentage conversion of PPS to BC was calculated as:

$$\%BC = \frac{m_1}{m_2} * 100$$

Where  $m_1$  is the starting mass of PPS and  $m_2$  is the mass of BC produced. The percentage conversion was 24% at  $700^\circ\text{C}$

### 2.3 Characterisation of Biochar and $\text{Fe}_2\text{O}_3$ -BC

The BC and Fe<sub>2</sub>O<sub>3</sub>-BC samples were characterised using Fourier transform infrared spectroscopy (FTIR), X-ray diffraction (XRD) analysis, and scanning electron microscopy (SEM) for surface area analysis.

### **2.3.1 Fourier-transform infrared spectroscopy (FTIR)**

Infrared red spectroscopy (FTIR 3000, WQF-520, attenuated) was used to identify the functional groups present in the synthesized samples of biochar before and after adsorption. The FT-IR studies were carried out in the 4000 to 400 cm<sup>-1</sup> wavenumber range. Background correction was done first and the dried solids were pressed with FTIR grade KBr and the pellets scanned 32 times using transmission mode with a resolution of 4 cm<sup>-1</sup>.

## **2.4 Adsorption Studies**

The adsorption properties of the synthesised Fe<sub>2</sub>O<sub>3</sub>-BC and BC were determined by application in aqueous solutions of known heavy metal (Pb) and dye (Methyl Orange) concentrations. A UV/VIS Spectrophotometer (Lasany Double Beam LI-2802) and FAAS (AA-6701F) were used for the measurement of Methyl Orange and Lead concentrations. Three replicates of different concentrations were prepared one for lead removal and the other for methyl orange removal. 1000 ppm stock solutions each of Lead and Methyl orange were prepared in 1 litre distilled water. Afterwards, solutions were diluted to different concentrations. The pH values of solutions were adjusted by addition of HCl and NaOH. Effects of pH, contact time, adsorbent dosage and adsorbate concentration on the adsorption of Pb and Methyl Orange (MO) was investigated through a series of experiments.

### **2.4.1 Effect of pH**

The effects of pH on adsorption of Pb were investigated at pH 2, 4, 10 and 12 using a 50 ml solution of 5 mg/L Pb, with 50 mg of Fe<sub>2</sub>O<sub>3</sub>-BC and BC. For MO dye the effect of pH on adsorption were investigated at pH 2, 4, 8, 10 and 12 using a 20 ml of 50 mg/L MO solutions and 50 mg of Fe<sub>2</sub>O<sub>3</sub>-BC and BC.

### **2.4.2 Effect of contact time**

The effect of contact time on Pb adsorption was studied by shaking 50 mg of (Fe<sub>2</sub>O<sub>3</sub>-BC and BC) for 15, 30, 60 and 90 minutes in a 50ml solution of 5 mg/L Pb. For MO, the effect of contact time was studied by shaking 50 mg of Fe<sub>2</sub>O<sub>3</sub>-BC and BC for 15, 30, 60, and 90 minutes in a 20ml solution of 50 ppm MO solution.

### **2.4.3 Effect of adsorbate concentration**

The effects of initial Pb concentration were studied using 5, 10, 15, and 20 mg/L of Pb solutions, for each adsorbent in and BC. The effect of initial dye concentration was studied using 50,100, 150, 200 and 250 mg/L MO solutions. The adsorbents for Pb and MO were 50 ml solution of 50 mg Fe<sub>2</sub>O<sub>3</sub>-BC and 20ml solution of 50 mg Fe<sub>2</sub>O<sub>3</sub>-BC respectively

### **2.4.4 Effect of adsorbent dosage**

For Pb, the effect of adsorbent dosage was investigated by separately shaking a 50 ml solution of 5 mg/L of Pb with 50, 100, 150 and 200 mg Fe<sub>2</sub>O<sub>3</sub>-BC for 30 minutes. The of adsorbent dosage on MO dye adsorption was investigated by separately shaking 50 mg/L solutions of MO dosage with 50, 100, 150, 200 and 250 mg Fe<sub>2</sub>O<sub>3</sub>-BC for 30 minutes.

The initial and equilibrium concentrations of Pb<sup>2+</sup> ions and MO in solutions were recorded and the amount adsorbed was calculated using the equations:

$$Q_e = \frac{V(C_i - C_e)}{m}$$

$$\% \text{ removal} = \frac{C_i - C_e}{C_i} * 100$$

Where  $C_i$  and  $C_e$  are the initial and equilibrium concentrations of Pb<sup>2+</sup> ions and MO in ppm,

$Q_e$  is the amount of Pb<sup>2+</sup> ions and MO adsorbed at equilibrium in mg/g,  $V$  is the volume of Pb<sup>2+</sup> and MO solutions (L) and  $m$  is the mass of BC and Fe<sub>2</sub>O<sub>3</sub>-BC in grams [11,38].

The Langmuir and Temkin equations were used to describe the equilibrium between the adsorbate and adsorbent represented as:

$$\frac{C_e}{Q_e} = \frac{C_e}{Q_{max}} + \frac{1}{Q_{max} * kl}$$

$$Q_e = \frac{RT}{b} \ln a C_e$$

Where  $Q_{max}$  and  $kl$  are the maximum adsorption capacity for the solid phase loading and the energy constant related to the heat of adsorption respectively. Plotting  $C_e/Q_e$  versus  $C_e$ , gives a straight line with  $Q_{max}$  and  $kl$  determined from the intercept and the slope of the graph respectively. Also a plot of  $Q_e$  versus  $\ln C_e$  gives a straight line [32].

### 3. RESULTS AND DISCUSSION

#### 3.1 FTIR Characterisation

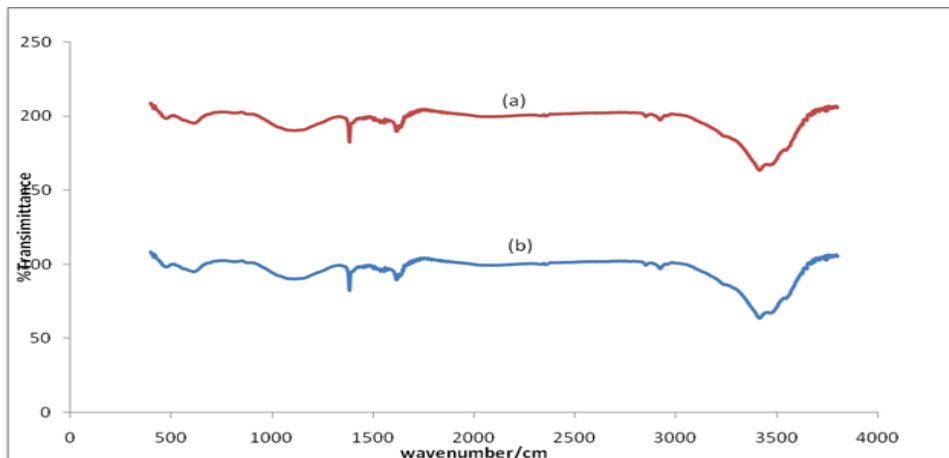


**Figure 1:** Fe<sub>2</sub>O<sub>3</sub>-BC FTIR Spectra (a) after adsorption and (b) before adsorption

Figure 1 shows -OH stretching as can be depicted from the pronounced peaks in the range of 3300-3500cm<sup>-1</sup>. Also present were -CH<sub>x</sub> stretching bands, 1600cm<sup>-1</sup> related to the aromatic structure, 1390 cm<sup>-1</sup>phenolics -OH, 830 cm<sup>-1</sup> alkene CH band, 600cm<sup>-1</sup> due Fe-O bond and 490cm<sup>-1</sup> regions with Fe<sub>2</sub>O<sub>3</sub>-BC. The 490 cm<sup>-1</sup> region with Fe<sub>2</sub>O<sub>3</sub>-BC show the presence of Iron oxide. This is in agreement with literature [11]. The major differences between the peaks before adsorption and after adsorptions were where the 1100cm<sup>-1</sup> peak broadened to stretch from 975- 1275cm<sup>-1</sup> corresponding to the MO fingerprint region [16]. This indicates the effect of heavy metal and dye addition.

### 3.3 Adsorption Experiment Results

#### 3.3.1 Effect of pH

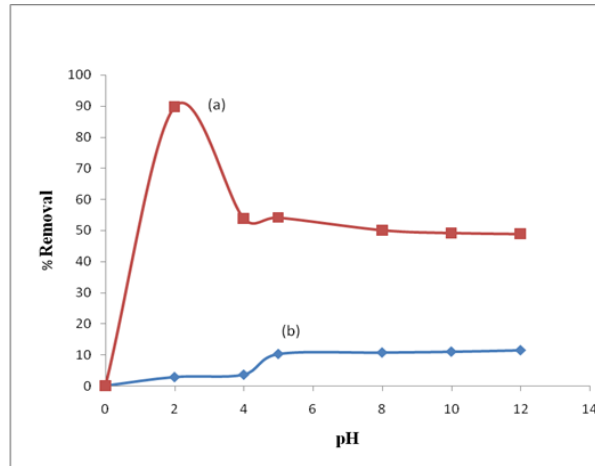


Figure 2: Effect of pH on MO removal, (a) using Fe<sub>2</sub>O<sub>3</sub>-BC and (b) using BC

Figure 2 shows that Fe<sub>2</sub>O<sub>3</sub>-BC had a highest percentage MO removal of 89.81% at pH 2, while BC had 11.53% at pH 12. This may prove that at pH 2; Fe<sup>3+</sup> is more effective in acidic conditions for the removal of MO. Fe<sup>3+</sup> ions with the combination of H<sup>+</sup> ions present at low pH provided the much needed cationic binding sites for anion MO.

#### 3.3.2 Effect of Contact Time

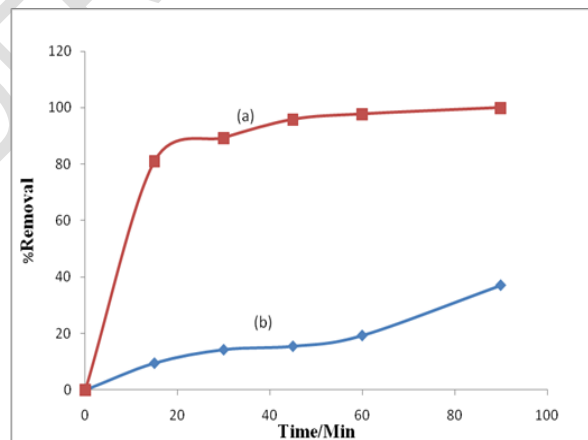
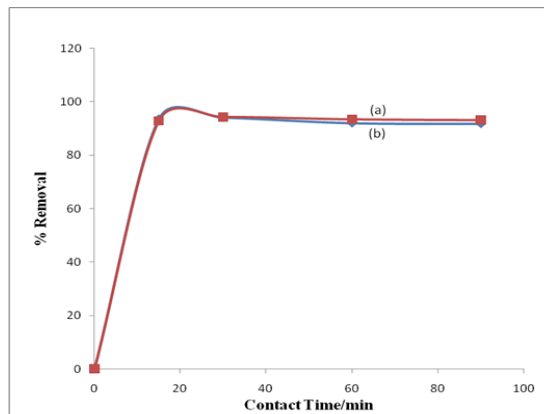


Figure 3: Effect of Contact Time on MO removal, (a) using Fe<sub>2</sub>O<sub>3</sub>-BC and (b) using BC

In Figure 3, the high rate of MO removal (90%) was witnessed in the first 15 minutes. Less than 50% of MO was removed by BC after 90mins. The rapid MO adsorption is attributed to

the presence of large number of surface sites initially and steadies thereafter [7]. Figure 4 below shows the effect of contact time on the adsorption of  $Pb^{2+}$ .



**Figure 4: Effect of Contact time on  $Pb^{2+}$  removal (a) using  $Fe_2O_3$ -BC and (b) using BC**

Figure 4 show that both adsorbents BC and  $Fe_2O_3$ -BC had 97% Pb removal in the first 15 minutes. The adsorptions were rapid for the first 15 minutes and gradually approached equilibrium between 30 and 90 minutes.

### 3.3.3 Effect of Adsorbate concentration

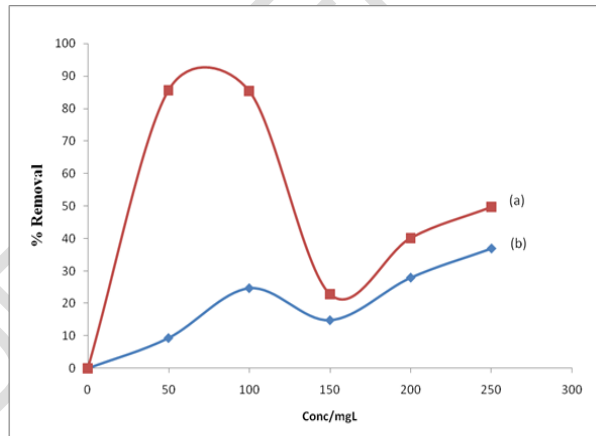


**Figure 5: Effect of Adsorbate concentration on MO removal (a) using  $Fe_2O_3$ -BC and (b) using BC**

In figure 5, 91% MO removal was achieved after the addition of MO concentration for  $Fe_2O_3$ -BC of 70 mg/L. There are fluctuations in MO percentage removal as the concentration is increased. The BC adsorbent gave a maximum of 37% after the addition of 200 mg/L MO. This is because the active binding sites were all occupied as the MO concentration is increased. After saturation no adsorptions were possible.



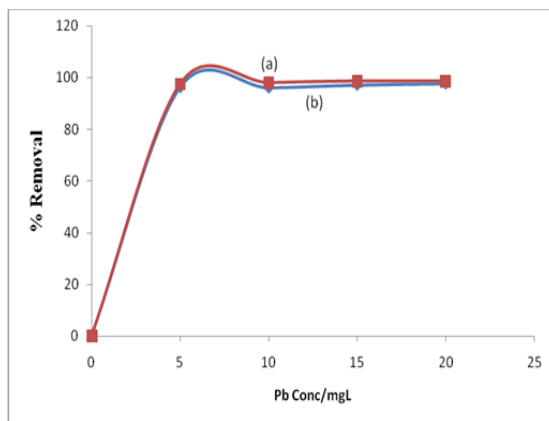


**Figure 6: Effect of Adsorbate concentration on Pb<sup>2+</sup> removal (a) using Fe<sub>2</sub>O<sub>3</sub>-BC and (b) using BC**

Figure 6 shows the optimum Pb<sup>2+</sup> concentration of 6.5 mg/L for both adsorbents with 100% Pb<sup>2+</sup> removal. The removal increased from 0 - 6.5 ppm. There was little effect of concentration after 6.5 mg/L.

### 3.3.4 Effect of Adsorbent dosage

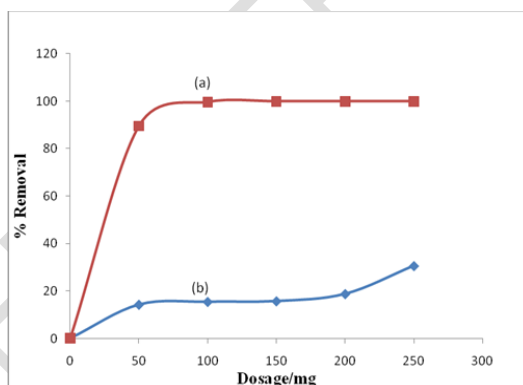


**Figure 2: Effect of Adsorbent dosage on MO removal (a) using Fe<sub>2</sub>O<sub>3</sub>-BC and (b) using BC**

In figure 7, 100mg of Fe<sub>2</sub>O<sub>3</sub>-BC adsorbent had a 100% removal of MO. The BC adsorbent after addition of 250 mg had a maximum removal of 30.61% though there was a sharp increase between 200 and 250 mg. This is in agreement with literature that at low pH, BC has few H<sup>+</sup> ions and at high pH more anions are predominantly present thereby hindering binding of MO onto the BC surface [30]. The Fe<sub>2</sub>O<sub>3</sub>-BC at low pH contained both Fe<sup>3+</sup> and H<sup>+</sup> ions which were available to adsorb the entire available MO in solution.

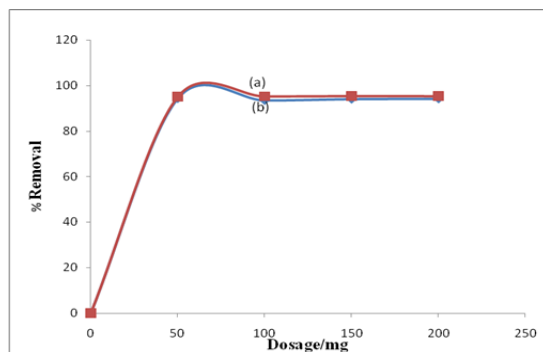


**Figure 3: Effect of Adsorbent dosage on Pb<sup>2+</sup> removal (a) using Fe<sub>2</sub>O<sub>3</sub>-BC and (b) using BC**

Figure 8 show that 100% of Pb<sup>2+</sup> ions removal was achieved on addition of 65mg of both adsorbents. There was rapid removal of Pb<sup>2+</sup> ions from 0-65 mg, followed by a sharp decline towards 100 mg and 200 mg. There were no major differences in adsorption capacities of both the adsorbents. Adsorption diminishes as the active sites are used up.

### 3.4 Adsorption Isotherms

#### 3.4.1 Langmuir Plots

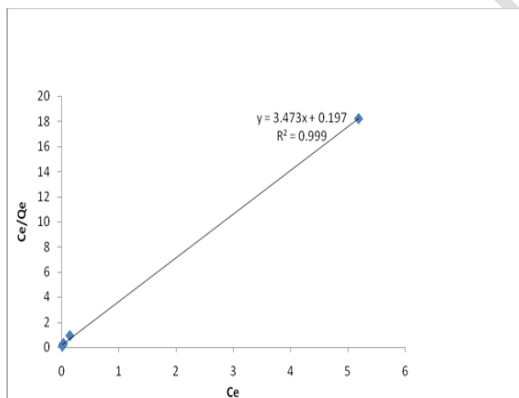


**Figure 4: Langmuir Plot for MO results**

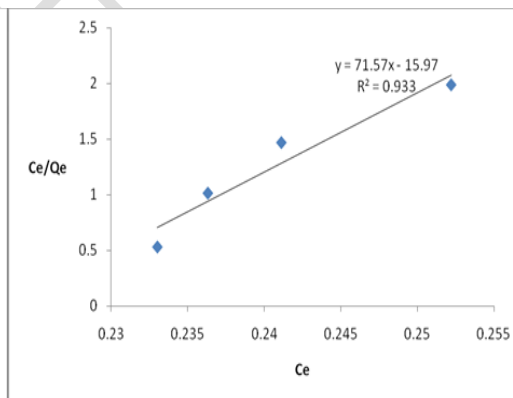


**Figure 10: Langmuir Plot for Pb<sup>2+</sup> results**

Figure 9 shows that the Langmuir isotherm and describes the adsorption of MO dye onto Fe<sub>2</sub>O<sub>3</sub>-BC with R<sup>2</sup> value of 0.999. The closeness of R<sup>2</sup> value to 1 indicates that the data obtained fits Langmuir Isotherm model of monolayer adsorption kinetics. The Fe<sub>2</sub>O<sub>3</sub>-BC nano-composite used can be said to have a series of distinct homogeneous sites available for binding the MO anions in solution. Figure 10 describes the sorption of Pb<sup>2+</sup> ions on the Fe<sub>2</sub>O<sub>3</sub>-BC with R<sup>2</sup> value of 0.933 also fits the Langmuir Isotherm well.

### 3.4.2 Temkin Plots

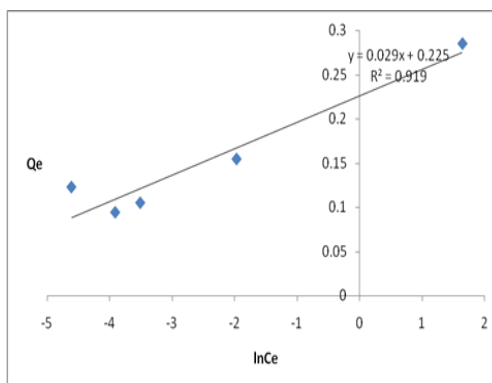


Figure 11: Temkin Plot MO results

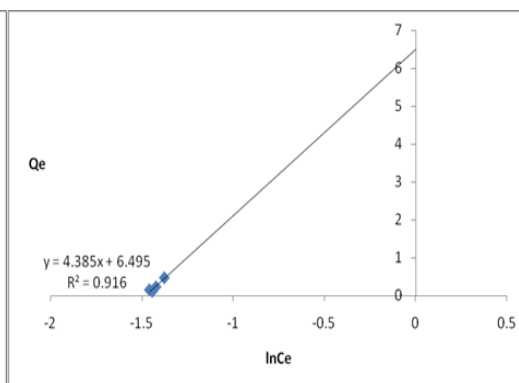


Figure 12: Temkin Plot Pb<sup>2+</sup> results

Figures 11 and 12 show the Temkin plot with  $R^2$  values of 0.919 and 0.916 for the sorption of MO onto Fe<sub>2</sub>O<sub>3</sub>-BC and Pb<sup>2+</sup> ions on the Fe<sub>2</sub>O<sub>3</sub>-BC respectively, fitting in the model that the heat of adsorption of all the molecules in the layer would decrease linearly rather than logarithmic with coverage.

## 4. CONCLUSION

Fe<sub>2</sub>O<sub>3</sub>-BC had highest percentage removal of 89.81% at pH 2 while BC had a highest of 11.55% at pH 12 of MO in solution. The dosage of 100 mg of Fe<sub>2</sub>O<sub>3</sub>-BC had 100% removal of MO and 250 mg BC achieved 30.61% removal in 30 minutes. The maximum concentrations were 70 ppm and 55 ppm respectively for Fe<sub>2</sub>O<sub>3</sub>-BC and BC adsorbents. In the removal of Pb<sup>2+</sup> ions in solutions both Fe<sub>2</sub>O<sub>3</sub>-BC and BC performances were almost similar with maximum removal of 97% in 30 minutes. 65 mg for both Fe<sub>2</sub>O<sub>3</sub>-BC and BC adsorbents had 100% removal. The adsorption performance of Fe<sub>2</sub>O<sub>3</sub>-BC is far much better than that of biochar in single aqueous solutions. Fe<sub>2</sub>O<sub>3</sub>-BC is an effective alternative adsorbent for Pb<sup>2+</sup> ions and methyl orange dye in aqueous solutions. There is need to perform further studies in order to find out the adsorption performance of Fe<sub>2</sub>O<sub>3</sub>-BC in binary and ternary solutions. The adsorption performance of Fe<sub>2</sub>O<sub>3</sub>-BC also needs to be evaluated on other common heavy metals and organic pollutants.

## REFERENCES

1. Abbas SH, Ismail IM, Mostafa TM, Sulaymon AH. Biosorption of heavy metals: a review. *Journal of Chemical Science and Technology*. 2014;3(4):74-102.
2. Abdel-Ghani NT, El-Chaghaby GA. Biosorption for metal ions removal from aqueous solutions: a review of recent studies. *Int J Latest Res Sci Technol*. 2014;3(1):24-42.
3. Ahluwalia SS, Goyal D. Microbial and plant derived biomass for removal of heavy metals from wastewater. *Bioresource technology*. 2007;98(12):2243-57.

4. Ahmad M, Rajapaksha AU, Lim JE, Zhang M, Bolan N, Mohan D, Vithanage M, Lee SS, Ok YS. Biochar as a sorbent for contaminant management in soil and water: a review. *Chemosphere*. 2014;1(99):19-33.
5. Al-Homaidan AA, Al-Houri HJ, Al-Hazzani AA, Elgaaly G, Moubayed NM. Biosorption of copper ions from aqueous solutions by *Spirulina platensis* biomass. *Arabian Journal of Chemistry*. 2014;7(1):57-62.
6. Alpat SK, Özbayrak Ö, Alpat Ş, Akçay H. The adsorption kinetics and removal of cationic dye, Toluidine Blue O, from aqueous solution with Turkish zeolite. *Journal of hazardous materials*. 2008;151(1):213-20.
7. Alsilaibi TM, Abustan I, Ahmad MA, Foul AA. Comparison of activated carbon prepared from olive stones by microwave and conventional heating for iron (II), lead (II), and copper (II) removal from synthetic wastewater. *Environmental Progress & Sustainable Energy*. 2014;33(4):1074-85.
8. Baker MN, Taras MJ. *The quest for pure water: The history of the twentieth century*, volume 1 and 2. Denver: AWWA. 1981.
9. Beesley L, Marmiroli M. The immobilisation and retention of soluble arsenic, cadmium and zinc by biochar. *Environmental pollution*. 2011;159(2):474-80.
10. Belaid KD, Kacha S, Kameche M, Derriche Z. Adsorption kinetics of some textile dyes onto granular activated carbon. *Journal of Environmental Chemical Engineering*. 2013;1(3):496-503.
11. Chaukura N, Murimba EC, Gwenzi W. Removal of Methyl Orange from Water using low-cost Biochar-Ferric Oxide Nano-composites derived from Pulp and Paper Sludge. *Appl. Water Sci*. 2016.
12. Chen B, Chen Z, Lv S. A novel magnetic biochar efficiently sorbs organic pollutants and phosphate. *Bioresource technology*. 2011;102(2):716-23.
13. Cortés-Martínez R, Martínez-Miranda V, Solache-Ríos M, García-Sosa I. Evaluation of natural and surfactant-modified zeolites in the removal of cadmium from aqueous solutions. *Separation Science and Technology*. 2004;39(11):2711-30.
14. Crittenden JC, Trussell RR, Hand DW, Howe KJ, Tchobanoglous G. *MWH's water treatment: principles and design*. John Wiley & Sons. 2012.
15. EPA, *The history of drinking water treatment*, Environmental Protection Agency, Office of Water (4606), Fact Sheet EPA-816-F-00-006, United States. 2000.
16. Goscińska J, Marciniak M, Pietrzak R. Mesoporous carbons modified with lanthanum (III) chloride for methyl orange adsorption. *Chemical Engineering Journal*. 2014;1(247):258-64.
17. Hamdaoui O. Batch study of liquid-phase adsorption of methylene blue using cedar sawdust and crushed brick. *Journal of hazardous materials*. 2006;135(1-3):264-73.
18. Hammami A, González F, Ballester A, Blázquez ML, Muñoz JA. Simultaneous uptake of metals by activated sludge. *Minerals Engineering*. 2003;16(8):723-9.
19. Huang H, Cao L, Wan Y, Zhang R, Wang W. Biosorption behavior and mechanism of heavy metals by the fruiting body of jelly fungus (*Auricularia polytricha*) from aqueous solutions. *Applied microbiology and biotechnology*. 2012;96(3):829-40.
20. Huang S, Lin G. Biosorption of Hg (II) and Cu (II) by biomass of dried *Sargassum fusiforme* in aquatic solution. *Journal of Environmental Health Science and Engineering*. 2015;13(1):21.
21. Kumar S, Loganathan VA, Gupta RB, Barnett MO. An assessment of U (VI) removal from groundwater using biochar produced from hydrothermal carbonization. *Journal of environmental management*. 2011;92(10):2504-12.
22. Mašek O, Budarin V, Gronnow M, Crombie K, Brownsort P, Fitzpatrick E, Hurst P. Microwave and slow pyrolysis biochar—Comparison of physical and functional properties. *Journal of Analytical and Applied Pyrolysis*. 2013;1(100):41-8.
23. McKay G, Allen SJ. Surface mass transfer processes using peat as an adsorbent for dyestuffs. *The Canadian Journal of Chemical Engineering*. 1980;58(4):521-6.

24. Motasemi F, Afzal MT. A review on the microwave-assisted pyrolysis technique. *Renewable and sustainable energy reviews*. 2013;1(28):317-30.
25. Mukherjee A, Zimmerman AR, Harris W. Surface chemistry variations among a series of laboratory-produced biochars. *Geoderma*. 2011;163(3-4):247-55.
26. Norton L, Baskaran K, McKenzie T. Biosorption of zinc from aqueous solutions using biosolids. *Advances in Environmental Research*. 2004;8(3-4):629-35.
27. Outwater A. *Water—A Natural History*. New Yor: Basic Book, a division of Harper Collins Publisher. 1996.
28. Pagnanelli F, Toro L, Veglio F. Olive mill solid residues as heavy metal sorbent material: a preliminary study. *Waste Management*. 2002;22(8):901-7.
29. Pandey S, Mishra SB. Sol-gel derived organic-inorganic hybrid materials: synthesis, characterizations and applications. *Journal of sol-gel science and technology*. 2011;59(1):73-94.
30. Pereira MF, Soares SF, Órfão JJ, Figueiredo JL. Adsorption of dyes on activated carbons: influence of surface chemical groups. *Carbon*. 2003;41(4):811-21.
31. Rich G, Cherry K. *Hazardous Waste Treatment Technology*, Pudvan Publ. Co., New York. 1987.
32. Shi B, Li G, Wang D, Feng C, Tang H. Removal of direct dyes by coagulation: The performance of preformed polymeric aluminum species. *Journal of hazardous materials*. 2007;8(143):567-74.
33. Siculus, Diodorus. "Library of History, volume III, Loeb Classical Library." (1939).
34. Wang J, Chen C. Biosorbents for heavy metals removal and their future. *Biotechnology advances*. 2009;27(2):195-226.
35. Wang S, Gao B, Zimmerman AR, Li Y, Ma L, Harris WG, Migliaccio KW. Removal of arsenic by magnetic biochar prepared from pinewood and natural hematite. *Bioresource technology*. 2015;1(175):391-5.
36. Yao Y, Gao B, Chen J, Zhang M, Inyang M, Li Y, Alva A, Yang L. Engineered carbon (biochar) prepared by direct pyrolysis of Mg-accumulated tomato tissues: characterization and phosphate removal potential. *Bioresource technology*. 2013;1(138):8-13.
37. Zhang M, Gao B, Varnosfaderani S, Hebard A, Yao Y, Inyang M. Preparation and characterization of a novel magnetic biochar for arsenic removal. *Bioresource technology*. 2013;1(130):457-62.
38. Zhang M, Gao B. Removal of arsenic, methylene blue, and phosphate by biochar/AlOOHnanocomposite. *Chemical engineering journal*. 2013;15(226):286-92.
39. Zhou Y, Gao B, Zimmerman AR, Chen H, Zhang M, Cao X. Biochar-supported zerovalent iron for removal of various contaminants from aqueous solutions. *Bioresource technology*. 2014;1(152):538-42.
40. Zhou Y, Gao B, Zimmerman AR, Fang J, Sun Y, Cao X. Sorption of heavy metals on chitosan-modified biochars and its biological effects. *Chemical Engineering Journal*. 2013;1(231):512-8.
41. Zhu D, Kwon S, Pignatello JJ. Adsorption of single-ring organic compounds to wood charcoals prepared under different thermochemical conditions. *Environmental science & technology*. 2005;39(11):3990-8.